Available online at www.sciencedirect.com

ScienceDirect

Physics Procedia 83 (2016) 1118 – 1129

Physics Procedia

9th International Conference on Photonic Technologies - LANE 2016

Experimental and simulative investigations of laser assisted plastic-metal-joints considering different load directions

Christoph Engelmann[a,*], Johannes Eckstaedt[a], Alexander Olowinsky[a], Mirko Aden[a], Viktor Mamuschkin[b]

[a]*Fraunhofer Institute for Laser Technology (ILT), Steinbachstraße 15, 52074 Aachen, Germany*
[b]*Chair for Technology of Optical Systems (TOS), Steinbachstraße 15, 52074 Aachen, Germany*

Abstract

Particularly in the automotive industry, the combination of dissimilar materials presents manufacturing engineering with major challenges. Notably, the adapted use of plastic and metal opens up further potential for weight savings. Directly and firmly bonding the two materials together fails, however, on account of the chemical and physical dissimilarity of plastic and metal. Since joining of plastics and metals nowadays is based on adhesive bonding, the joint is weak and underlies ageing processes. A promising approach to overcome these problems is a laser based two-step process. In the first process step laser radiation is applied to generate microstructures on the surface of the metallic joining partner. In the subsequent laser joining process, the plastic is molten and interlocked into the microstructures after curing.

The mechanical strength of the joint depends strongly on the load direction and can be influenced by the geometry and arrangement of microstructures. These influencing factors are investigated for three different load directions (tensile shear, tensile and peel) by experiments and by structural mechanics simulations.

Peer-review under responsibility of the Bayerisches Laserzentrum GmbH

Keywords: laser joining; lightweight; plastic-metal-joints; microstructuring; structural mechanics simulations; form locking

* Corresponding author. Tel.: +49-241-8906-217 ; fax: +49-241-8906-121 .
E-mail address: christoph.engelmann@ilt.fraunhofer.de

Peer-review under responsibility of the Bayerisches Laserzentrum GmbH
doi:10.1016/j.phpro.2016.08.117

1. Introduction

Since nowadays one of the greatest challenges for automobile manufacturers is to slow down energy consumption and emissions of their cars. In the recent years, the European Commission passed for example new laws limiting the CO_2 emissions of new vehicles. These laws require that new cars, which are registered in Europe, do not emit more than an average of 130 g CO_2/km by 2015 and 95 g CO_2/km by 2020. If the average CO_2 emissions of a manufacturer's fleet exceed its limit value, the manufacturer has to pay penalty payments for each registered car [European Commission (2009)].

In this context the automotive industry is increasingly interested in a smart material mix, which enables lightweight construction. In order to save weight, the combination of different working materials, such as plastics and metals, is a mandatory requirement. While plastics are characterized by a nearly infinite number of forming possibilities, a low weight and favorable price, metals can withstand, thanks to their mechanical properties, significantly higher mechanical loads. A firm and direct bond between metal and plastic fails due to their chemical and physical differences. Nowadays joining of plastics and metals is mainly based on adhesive bonding. A promising approach to overcome problems with adhesive bonding like ageing processes or long cycle times is a laser based two-step process to join these dissimilar materials.

2. Laser based process chain for plastic-metal joints

The laser based process chain is shown in Fig. 1 and consists of a microstructuring process on first stage to generate microstructures on the metal surface. In a second laser based process the thermoplastic material is melted and by external clamping the plasticized material is pressed into the generated microstructures and forms after curing a mechanical interlocking between both materials [Holtkamp et al. (2012)].

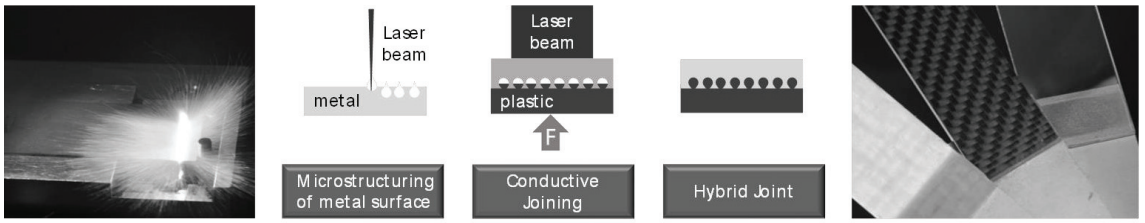

Fig. 1. Laser based process chain.

For the metal surface treatment as first process step, a high speed laser microstructuring process is applied, which is a productive way to realize fast cycle times needed for efficient production processes. A fast beam movement is realized by a galvometric scanning system, which allows scanning variable patterns on the metal surface. Because the process is based on a combination of sublimation and melting, the processing time is much shorter compared to conventional structuring processes [Engelmann et al. (2013), Heckert & Zaeh (2014), Rodríguez-Vidal et al. (2014)]. Due to the high intensity of the beam, metal material is sublimated in the center of the microstructure and the resulting evaporation pressure ejects the surrounding melt from the structure bottom over the edges towards the surface, where some parts of it can solidify. The structuring process is repeated to achieve an undercut structure since more and more generated melt recasts on the surface and on the edges of the structure.

The subsequent thermal joining process is realized by conductive joining. The metal surface is heated by laser radiation and by means of heat conduction the plastic is molten at the interface between both materials. The plasticized material expands and moves into the generated structures by an external clamping force. For a firm bond, the plasticized material has to flow into the generated structures, which have an undercut geometry, and to harden there. The laser based process chain for hybrid joints is very flexible and can be adapted to different thermoplastic materials and metals [Engelmann et al. (2015a)].

3. Experimental set-up

3.1. Laser microstructuring process of metal surface

The laser source utilized for the laser microstructuring process is a water cooled IPG Photonics YLS-1000-SM, 1000 W continuous wave single-mode fiber laser ($M^2 < 1.07$), operating at 1064 nm wavelength. The beam source is portable and of simple automation, and due to the high quality of the laser beam the system is ideal for joining, micro-machining, cutting and welding applications. The laser beam is guided through an optical fiber into an Instelliscan 25 scanhead, which deflects the laser beam on the metal surface. The metal is positioned in a device within the scan field to ensure reproducible patterns on metal surface. A cross-jet with pressured air prevents the optics from contamination by process emissions. The focusing F-theta optics has a focal length of 330 mm creating a focal radius of 20 µm. The system set-up is depicted in Fig. 2.

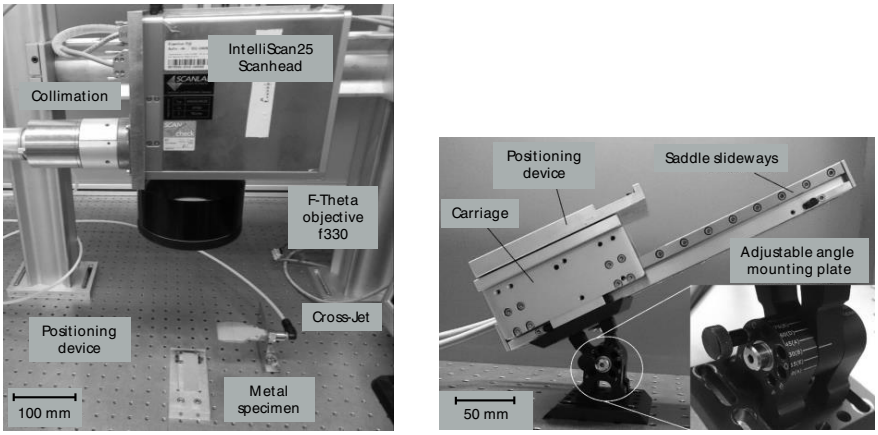

Fig. 2. System set-up laser microstructuring without (left) and with an angle of incidence (right).

To enable an incident angle of the microstructures, the positioning device is mounted on an adjustable angle plate (see Fig 2, right picture). Additionally the positioning device is mounted on a saddle slideways, which can be moved for defined structure distances working for each microstructure always in focus of the laser beam.

3.2. Laser conductive joining process

The utilized laser system for conductive joining process is a Laserline GmbH LDM 3000-100, 3000 W continuous wave diode laser, operating at 1018 nm wavelength. The laser beam is guided through an optical fiber into a zoom homogenizer optics device (Laserline GmbH) with a focal length of 250 mm shown in Fig. 3. The zoom optics allows the flexible forming of the laser beam into a rectangular shape with dimensions between 5x5 mm² and 30x16 mm² spot sizes. In order to apply a joining force and to fix the sample arrangement, a pneumatic clamping device with a specimen fixture is introduced. Plastic and metal specimens are placed overlapping inside the fixture and pressed with the pneumatic lifting cylinder against a clamping frame. The specimens are irradiated through the clamping frame from the metal side. The spot size is adapted to the bonding areas of the different test specimens allowing a simultaneous laser joining process with the two parameters laser power and irradiation time.

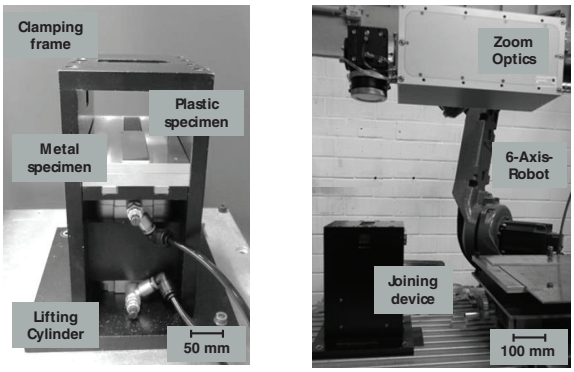

Fig. 3. System set-up laser conductive joining.

3.3. Test specimen and test procedure

The mechanical properties of the hybrid joints are tested with a multi-purpose testing machine Z100 from Zwick GmbH & Co. KG. For tensile shear tests a force is applied parallel to the joining area and the breaking force is measured according to DIN EN 1465. The samples are fixed between the clamping jaws, which have a distance of 80 mm between each other (Fig. 4). The testing speed is set to 50 mm/min. For tensile and peel tests a force is applied perpendicular to the joining area and the breaking force is recorded according to DIN EN ISO 527 and DIN EN ISO 11339. The distance between the clamping jaws is fixed for both tests to 25 mm, the testing speed is set also to 50 mm/min.

For each evaluated parameter for tensile, tensile shear and peel load, five samples are tested destructively. The dimensions of the three different test specimens are shown in Fig. 4. The thickness of utilized metal material (stainless steel 1.4301) is 1 mm and 2 mm thick plastic material for tensile shear and peel specimens and 4 mm for tensile specimens (Polycarbonate, Makrolon®). The bonding area for tensile shear specimen is 5x30 mm², for tensile specimen 25x4 mm² and 15x30 mm² for peel specimen.

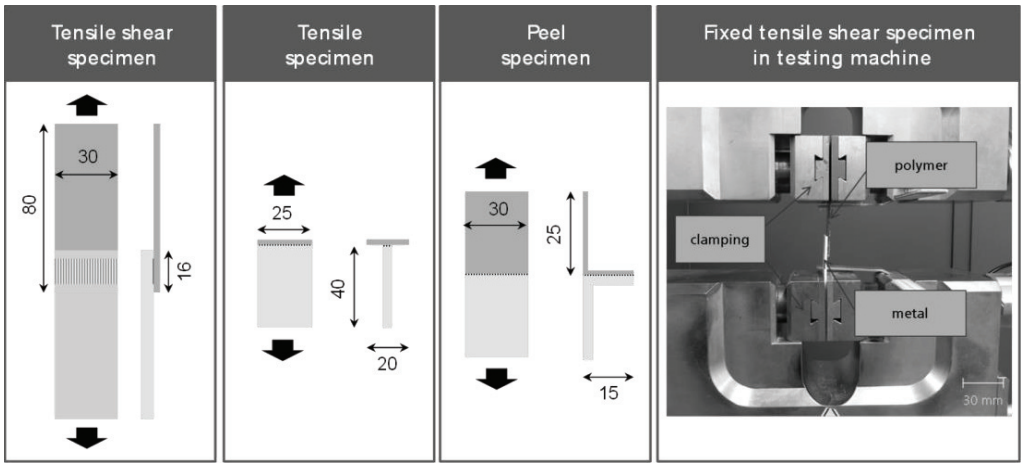

Fig. 4. Dimensions of test specimens and testing machine.

4. Experimental results

The metal surface is treated with different process parameters for all test specimens to evaluate influencing factors on resulting strength of the dissimilar joint for different load directions. The basic parameters, which are available for the microstructuring process, are summarized in Table 1.

Table 1. Parameters for microstructuring process.

Parameter	Acronym	unit
Laser power	P	W
Scan speed	v	m/s
Number of repetitions	N	#
Structure distance	b	µm
Incident angle	α	°

To evaluate the influence of different shapes of the microstructure, geometric parameters are introduced in Fig. 5. All microstructured metal plates without an incident angle (α=0°) are treated with a laser power of P=750 W and a scan speed of v=10 m/s, the process is repeated for each microstructure four times (N=4). If the microstructuring process is done under an incident angle above α= 15°, the number of repetitions is raised to achieve a suitable structure depth due to a higher reflection of the laser beam. The number of repetitions are N=7 for α=30°, N=6 for α=45° and N=5 for α= 60°, scan speed, laser power, structure distance and structure orientation are kept constant for all microstructured metal specimens under an angle of incidence (P=750 W; v=10 m/s; b= 200 µm; linear orientation).

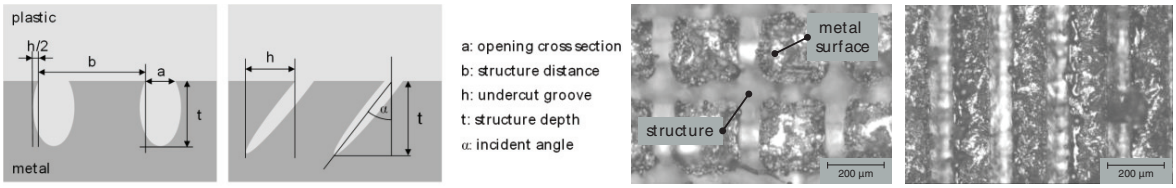

Fig. 5. Analyzed geometric parameters of the microstructure (left) and different structure orientations (right).

The structure orientation (pattern on the metal surface) in form of linear and crossed microstructure lines is shown in Fig. 5 in the right picture. In previous studies was investigated, that there is no difference for tensile shear strength of the joint, if the microstructures are arranged lateral or perpendicular to load direction [Engelmann et al. (2015b)]. In this study linear microstructures are arranged perpendicular to tensile shear and peel stress direction.

All test specimens are joined in a simultaneous laser joining process with the following parameters:

- Tensile shear specimen: Spot size A=5x30 mm²; Laser power P=750 W; Irradiation time T=1,5 s
- Tensile specimen: Spot size A=5x25 mm²; Laser power P=700 W; Irradiation time T=1,5 s
- Peel specimen: Spot size A=15x30 mm²; Laser power P=1350 W; Irradiation time T=1,5 s

4.1. Influence of structure distance on joint strength

The microstructured surface of the metal differs with 5x30 mm² for tensile shear, 25x4 mm² for tensile and 15x30 mm² for peel specimens. If the distance between adjacent structures is varied for a constant microstructured area, the total number of microstructures on the surface also varies. The influence of different structure distances for the three different load directions is shown in Fig. 6. The total amount of microstructures on the surface is halved from each pillar to the next.

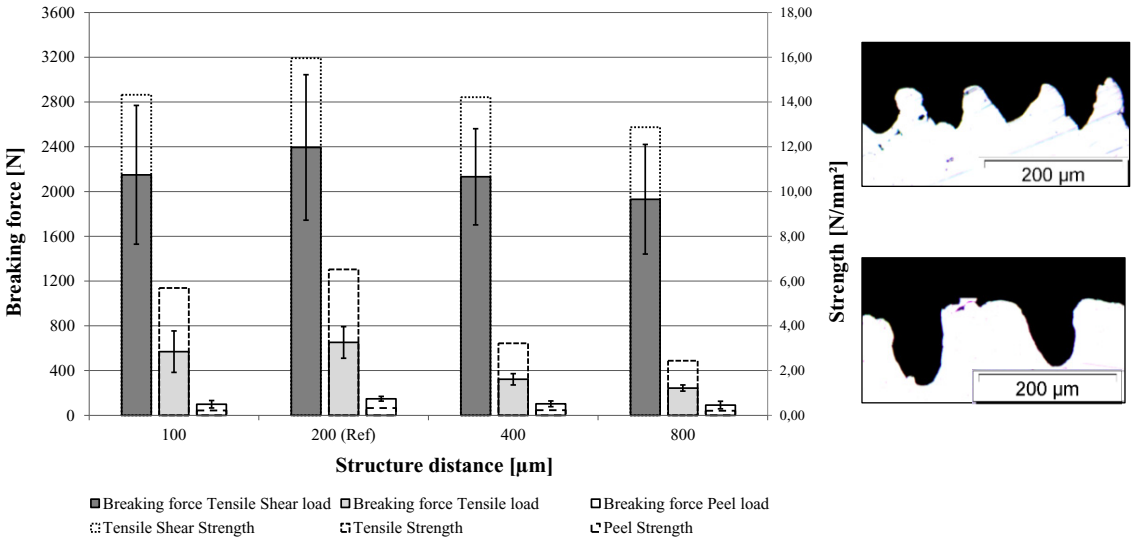

Fig. 6. Evaluated breaking forces and correspondant strength values for different structure distances and load directions.

If the structure distance is enlarged from 100 to 200 µm, the resulting breaking force is increased for all load directions. The cross sections in Fig. 6 (right pictures) for these two structure distances show for 100 µm distance varying shapes of the microstructures with a big opening cross section width and a lower structure depth compared to the microstructures with 200 µm structure distance. Because the structures are too close together at 100 µm structure distance, the formation of the geometry is influenced by adjacent structures. If the structure distance is raised to 400 or 800 µm, the resulting breaking force is reduced due to the fact that a minor number of structures are located in the metal surface [Amend et al. (2014)].

To be able to compare the next influencing factors, a reference structuring parameter (Ref) is introduced for all test specimens with the following parameters: P= 750 W; v =10 m/s; N =4; b= 200 µm; α= 0°; linear orientation. The highest joint strength for the reference is achieved for tensile shear load (15.96 N/mm²), followed by tensile load (6.52 N/mm² (reduction 59,15%)) and peel load (0.33 N/mm² (reduction 97,93%)). These first results show, that due to the high differences in values between these three load directions, hybrid components should be designed to ensure mainly shear load for the joint.

4.2. Influence of structure orientation on joint strength

Next, the influence of different structure orientations is evaluated. The total length of all structures included in the joining area equals for a linear arrangement of the microstrctures with a structure distance of 200 µm (400 µm) compared to a crossed orientation with a distance of 400 µm (800 µm).

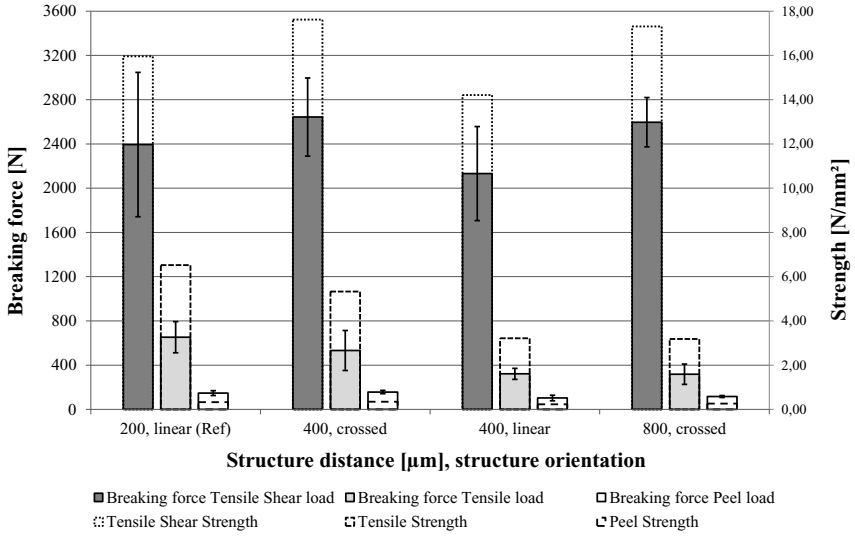

Fig. 7. Evaluated breaking forces and correspondant strength values for different structure orientations and load directions.

For tensile shear and peel test specimens the breaking forces can be raised, if crossed microstructuring patterns are applied compared to linear orientations (see Fig. 7). Another advantage is a minor standard deviation of the resulting breaking forces. The main reason for this improvement is a much higher depth of the microstructures at crossing points. The average depth of the reference structure is 130 µm and 90 µm for a structure distance of 400 µm. At crossing points, where the number of repetitions is duplicated, the resulting structure depth is 240 µm.

For tensile test specimens the breaking force is reduced and the standard deviation is increased by a crossed structure orientation. The crossing points are mainly leading to this decrease of strength, because there is a big opening cross section width with no undercut groove at these points. It is obvious that an undercut groove is mandatory to transfer tensile forces between the dissimilar materials. Overall, the results indicate that the pattern of the microstructures on the metal surface must be adapted to load directions to achieve a homogeneous stress distribution in a final part.

4.3. Influence of inclined microstructures on joint strength

The last evaluated influencing parameter is an incident angle of the microstructures. The measured breaking forces for nine different angles are depicted in Fig. 8 for tensile shear load direction. An incident angle is defined negative, if the geometry of the microstructures conduct like barbs in load direction, shown in the cross sections in Fig. 8.

Compared to the reference, the breaking force can be raised by any tested angle of incidence. The undercut groove can be raised by microstructuring under an angle of incidence compared to the reference (see Fig. 8). The curve progression is for positive and negative angles of incidence quite comparable. In most cases, a negative angle achieves a higher breaking force compared to the same positive angle. It is obvious, that the resulting breaking force depends on the dimension of the undercut groove [Rösner (2014), Schricker et al. (2014)]. If a sufficient structure depth is achieved, the breaking force cannot be raised by an increasing depth at a constant level of undercut groove (see incident angles ± 30° compared to ± 45°). The parameter with the highest resulting breaking force for tensile shear stress is P= 750 W; v= 10 m/s; N= 6; b= 200 µm; α= -45°; linear orientation achieving a breaking force of 3.27 kN.

Fig. 8. Evaluated breaking forces for different incident angles with applied tensile shear load.

Fig. 9 gives an overview over the influence of an incident angle of microstructures on resulting breaking force and strength for all evaluated load directions. Analogous to presented results in Fig. 8 for tensile shear load, nine different angles are evaluated. Like before defined is an incident angle negative, if the geometry of microstructures conduct like barbs in load direction. This is the case for tensile shear and peel load, but in case of tensile load there is no difference between a positive or a negative angle. For that reason only positive angles are performed in Fig. 9. The strength of the joint can be raised by any tested angle of incidence for all investigated load directions compared to the reference. Main reason for the increased strength is a higher undercut groove of the microstructures. For tensile shear load the highest breaking force is achieved for an angle of α= -45° with 3.27 kN, which corresponds to a tensile shear strength of 21.8 N/mm². The highest breaking force for tensile load is achieved for an angle of α= 45° with 1.14 kN, which corresponds to a tensile strength of 11.37 N/mm². For peel load the highest breaking force is achieved for an angle of α= -30° with 0.31 kN breaking force, which corresponds to a peel strength of 0.69 N/mm². The geometry of microstructures for peel specimens are very different to the geometry of tensile shear specimens for an incident angle of α= ±45° regarding structure depth (113.2 µm compared to 143.6 µm) and undercut groove (23.7 µm compared to 106.4 µm). Both values are significantly smaller for peel specimens, causing different curve progressions. A possible reason for these differences could be a wrong positioning of the metal components or a incorrect adjustment of the angle of incidence.

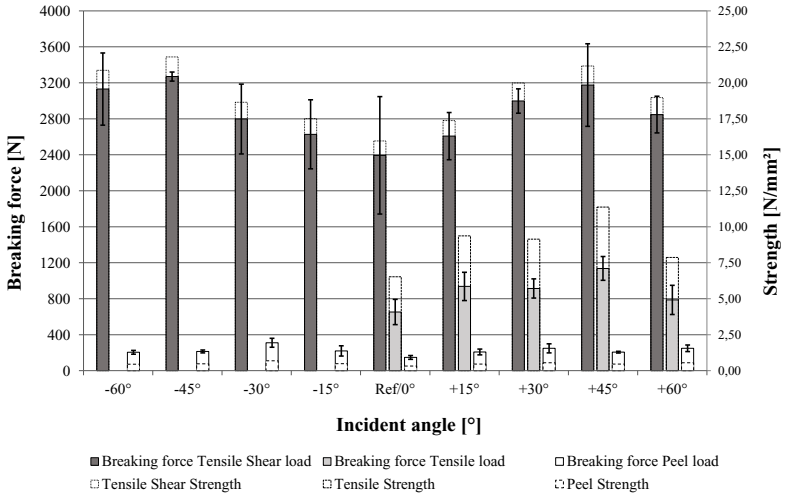

Fig. 9. Evaluated breaking forces and correspondant strength values for different incident angles and load directions.

5. Simulative results

For a theoretical investigation of influencing factors for the dissimilar joint, structural mechanics simulations of the join behavior are performed as well. The influence of different structure geometries and amount of structures on bonding area are investigated hereafter using a FEM-solver of the structural mechanics equations. Furthermore different load directions are applied.

The joined components will respond to an applied force by stress and deformation. The stress-strain dependence on the force is described by the equations of structural mechanics. In the presented simulations a linear stress-strain dependence of an isotropic-elastic material is assumed (Hooks law). The simulations are carried out using Comsol® Multiphysics software. The used physical properties for the simulation are compiled in Table 2 for plastic and metal.

Table 2. Physical properties of evaluated material combination.

Material	ρ [kg/m³]	E [GPa]	η [-]
Polycarbonate	1200	2.4	0.35
Steel AlSi 4340	7850	205	0.28

First, the geometry of the structures has to be modelled for a simulative approach. According to Fig. 10 the following geometric parameters are chosen to characterize the shape of a microstructure using Comsol® Multiphysics software. Next, a computational mesh has to be generated to be able to use a FEM solver.

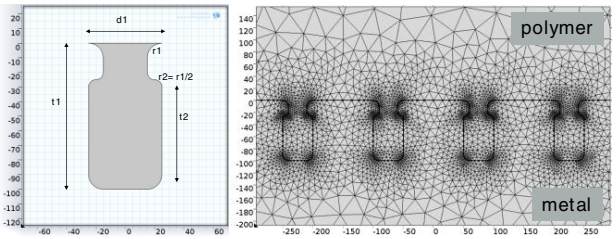

Fig. 10. Selected geometric parameters to characterize the microstructure (left) and computational mesh (right) for FEM solver.

The mesh is automatically adjusted by the software to typical dimensions and curvatures. On this mesh a stationary solution of the linear structural mechanical equations is obtained. For the evaluation of different influences the distribution of van mises stress is calculated and the maximum is analyzed. For all simulations the thickness of metal and plastic is 1 mm.

At first the influence of a higher number of structures is simulated for tensile shear and peel load direction. The dimensions of a single microstructure are: t1= 100 µm; t2=60 µm; d1= 50 µm; r1= 10 µm and r2= 5 µm. A tensile shear test is simulated with a load of 1 kN and a peel test with a load of 0.2 kN. The maximum of van mises stress for tensile shear load is 35 N/mm² for five structures and 23 N/mm² (reduction 34.39%) for ten structures (see Fig. 11). A higher amount of microstructures lead to a decrease of max. van mises stress due to the distribution of stress on more structures. The biggest stresses are located for both simulations at first and last microstructure shown in the scheme in Fig. 11, which is already known from adhesive bonding [Rasche (2012)]. But even the other microstructures in between are loaded with stress as Fig. 11 shows.

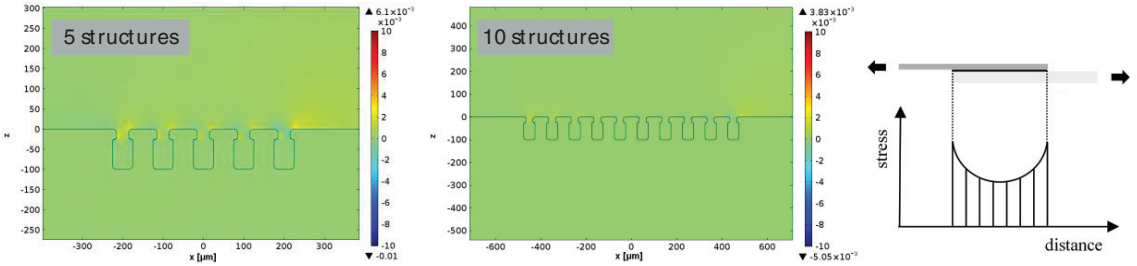

Fig. 11. Volumetric stretching of plastic for five (left) and ten (middle) microstructures for 1 kN tensile shear load and scheme of stress distribution.

For peel load the maximum of van mises stress is 45 N/mm² for five structures and 39 N/mm² (reduction 13.33%) for ten structures (see Fig. 12). It is obvious, that for peel load only the first and second structures experience significant stress, shown also in the scheme. One can conclude that for this load direction the join can bear less force than under tensile shear or tensile load direction, because for these more structures are loaded with stress (more homogeneous stress distribution, see Fig. 11). The maximum stretching and, therefore, tension reduces with a duplication of structures about 13.33% for peel load, while for tensile shear load this value is about 34,39%.

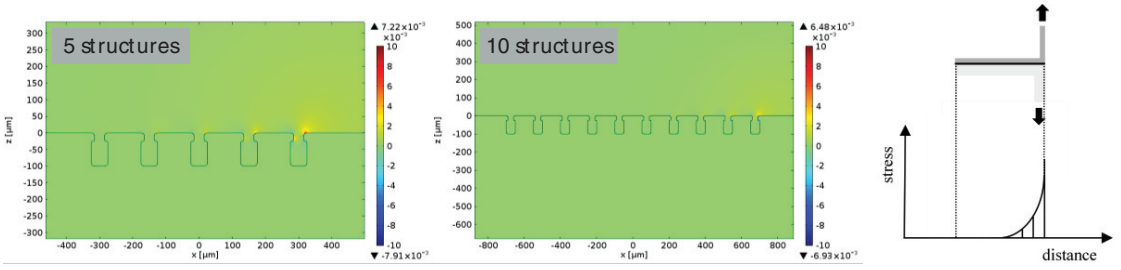

Fig. 12. Volumetric stretching of plastic for five (left) and ten (right) microstructures for 0.2 kN peel load and scheme of stress distribution.

Next, the influence of structure depth and width on van mises stress is evaluated. The left microstructures in Fig 13 show the same geometric parameters as described above, the microstructures in the middle of the figure have a halved width d1 to 25 µm. The halved width causes an increase of max. van mises stress to 44 N/mm² (increase +25,71%). The right microstructures in Fig. 13 have a halved structure depth t1 to 50 µm compared to the left. The decreased depth causes an increase of max. van mises stress to 59 N/mm² (increase +68,57%). The simulations show a higher influence on resulting stress by the depth of the microstructure compared to the microstructure width. The dependence between structure depth and resulting breaking force has been found out in the experiments as well, as long as a sufficient depth is not exceeded (see Fig. 8). The influence of different structure widths is subject to ongoing experimental investigations.

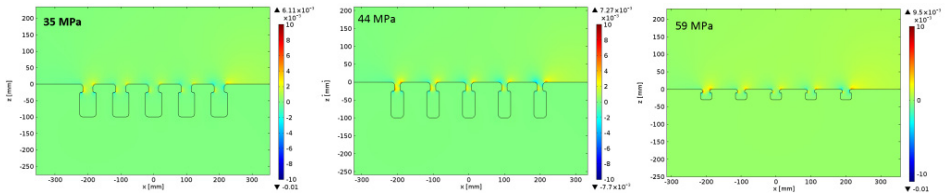

Fig. 13. Volumetric stretching of plastic for five microstructures with different shapes (Refence (left), halved width (middle) and halved depth (right)) for 1 kN tensile shear load.

6. Summary and Outlook

The described laser assisted process chain allows a flexible and fast microstructuring and conductive joining process to join thermoplastic plastics to metals. The connection strength depends in addition to structuring and joining parameters strongly on the applied load direction. The highest evaluated strength for tensile shear load has been 21.8 N/mm², for tensile load 11.37 N/mm² (reduction 47,8%) and 0.69 N/mm² for peel load (reduction 96,8%) for the used material combination. These high differences in values between the three load directions show, that hybrid components should be designed to ensure mainly tensile and tensile shear stress for the joint.

For every load direction, strength was increased by incident angles of the microstructures compared to the reference. The increase of strength was mainly achieved by a bigger undercut groove and a higher structure depth. Furthermore an influence on the joints perforemance was found out for different structure distances and structure orientations.

At last a simulative approach of the joint has been introduced, based on linear structural mechanics. The presented results show, how the strength of the joint is influenced by a higher amount of structures or different geometries of the structures for different load directions. Therefore, the simulations should be used to investigate how a certain geometric design will be applicable or has to be changed. Furthermore in ongoing investigations a close comparison between simulation model and experimental results has to be made to evaluate and optimize the model.

Acknowledgements

The work presented here is financed within the European joint projects »PM-Join« funded in the Seventh Framework Programme under grant agreement no. 309993 and »FlexHyJoin« funded in Horizon 2020 research and innovation program under grant agreement no. 677625. The authors thankfully acknowledge its financial support.

7. References

European Parliament and Council, 2009. Regulation (EC) No 443/2009 of 23 April 2009 setting emission performance standards for new passenger cars as part of Community's integrated approach to reduce CO2 emissions from light-duty vehicles.

J. Holtkamp, A. Roesner, A. Gillner, 2009. Advances in hybrid laser joining, International Journal of Advanced Manufacturing Technology, Springer-Verlag, pp. 923-930. London.

C. Engelmann, A. Rösner, A. Olowinsky, V. Mamuschkin, 2013. Lasermikrostrukturen zum lasergestützen Fügen von Kunststoff und Metall, DVS-Congress. Essen.

A. Heckert, M. Zaeh, 2014. Laser Surface Pre-treatment of Aluminium for Hybrid Joints with Glass Fibre Reinforced Thermoplastics, Physics Procedia 56, pp. 1171 – 1181.

E. Rodríguez-Vidal, J. Lambarri, C. Soriano, C. Sanz, G. Verhaeghe, 2014. A combined experimental and numerical approach to the laser joining of hybrid Polymer – Metal parts, Physics Procedia 56, pp. 835 – 844.

C. Engelmann, K. van der Straeten, 2015a. Laserbasierte Fügeverfahren, Photonik im Leichtbau, Lightweight design, Issue 2/2015, pp. 10-15.

C. Engelmann, K. van der Straeten, A. Olowinsky, V. Mamuschkin, 2015b. Laserbasierte Fügeverfahren für faserverstärkte Kunststoffe DVS-Congress. Nürnberg.

P. Amend, C. Mohr, S. Roth, 2014. Experimental Investigations of Thermal Joining of Polyamide Aluminum Hybrids Using a Combination of Mono- and Polychromatic Radiation, Physics Procedia 56, pp. 824 – 834.

A. Rösner, 2014. Laserbasiertes Fügeverfahren zur Herstellung von Kunststoff-Metall-Hybridbauteilen, PhD Thesis, University Aachen.

K. Schricker, M. Stambke, J. P. Bergmann, K. Bräutigam, 2014. Macroscopic Surface Structures for Polymer-Metal Hybrid Joints manufactured by Laser Based Thermal Joining, Physics Procedia 56, pp. 782 – 790.

M. Rasche, 2012. Handbuch Klebtechnik, Carl Hanser Verlag, p. 599.